HHS Public Access

Author manuscript

Chem Res Toxicol. Author manuscript; available in PMC 2018 May 15.

Published in final edited form as:

Chem Res Toxicol. 2017 May 15; 30(5): 1127–1133. doi:10.1021/acs.chemrestox.6b00439.

Replicative Bypass Studies of α-Anomeric Lesions of 2′-Deoxyribonucleosides *in Vitro*

Nicole L. Williams[†], **Nicholas J. Amato**[‡], and **Yinsheng Wang**[*,†,‡]

[†]Environmental Toxicology Graduate Program, University of California, 501 Big Springs Road, Riverside, California 92521-0403, United States

[‡]Department of Chemistry, University of California, 501 Big Springs Road, Riverside, California 92521-0403, United States

Abstract

Genomic integrity is constantly challenged by a variety of endogenous and exogenous DNA damaging agents, which can lead to the formation of 10^4–10^5 DNA lesions per cell per day. Reactive oxygen species (ROS) represent a major type of DNA damaging agent. Specifically, a hydroxyl radical can attack the C1′ position of 2-deoxyribose, and the ensuing carbon-centered radical, if improperly repaired, can cause the inversion of stereochemical configuration at the C1′ to give α-anomeric lesions. In this study, we assessed the replicative bypass of α-dA, α-dT, α-dC, and α-dG in template DNA by conducting primer extension assays with the use of purified translesion synthesis DNA polymerases. Our results revealed that human polymerase (Pol) η, but not human Pol κ, Pol ι, or yeast Pol ζ, was capable of bypassing all of the α-dN lesions and extending the primer to generate full-length replication products. Data from steady-state kinetic measurements showed that Pol η was the most efficient in inserting the correct nucleotides opposite the modified nucleosides, with the relative efficiencies of nucleotide incorporation following the order of α-dA > α-dG > α-dT > α-dC. Additionally, human Pol η was found to misincorporate dTMP opposite α-dT and dCMP opposite α-dC at frequencies of 66% and 24%, respectively, whereas α-dA and α-dG were weakly miscoding. These findings provided important knowledge about the effects these α-dN lesions have on the fidelity and efficiency of DNA replication mediated by human Pol η.

Graphical abstract

[*]Corresponding Author: Tel: 951-827-2700. Fax: 951-827-4713. Yinsheng. Wang@ucr.edu.
ORCID: Yinsheng Wang: 0000-0001-5565-283X

Supporting Information: The Supporting Information is available free of charge on the ACS Publications website at DOI: 10.1021/acs.chemres-tox6b00439. Standing-start primer extension and steady-state kinetic assay results (PDF)

Notes: The authors declare no competing financial interest.

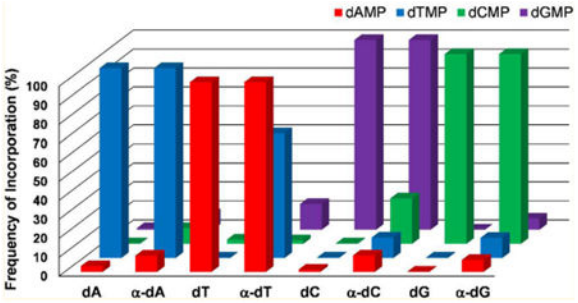

Introduction

Over one hundred years ago scientists noticed that organisms with higher metabolic rates often exhibited shorter life spans, and we have just started to unveil the principles behind this phenomenon.[1] Many theories have been proposed throughout the years, but the underlying molecular mechanisms of aging remain largely unclear. In the free radical theory of aging, it was argued that oxygen radicals could be generated in cells and result in damage.[2] After many years of research, the discovery of superoxide dismutase, whose main function is to remove superoxide anions, supports this theory.[1] Today, oxidative DNA damage is known to be associated with aging as well as the development of many human diseases including neuro-degeneration and cancer.[2–5]

Damage to cellular DNA by reactive oxygen species (ROS) represents a major type of DNA damage and is generally unavoidable due to ubiquitous exposure to various exogenous and endogenous agents.[1,6] ROS encompass a variety of chemical species including superoxide anion, hydroxyl radical, and hydrogen peroxide which are capable of inducing modifications to cellular proteins, lipids, and DNA.[1] For example, the hydroxyl radical can abstract a hydrogen atom from each of the five carbon atoms of the 2-deoxyribose to generate carbon-centered radicals. If not properly repaired, the radicals formed at the C1′, C3′, and C4′ positions can result in the inversion of stereochemical configuration at these carbons, thereby giving rise to epimeric 2-deoxyribose lesions.[7] These include the α-anomeric nucleosides emanating from such inversion at the C1′ position.[7]

The formation of α-dN lesions has been demonstrated in isolated DNA *in vitro* and in mammalian tissue DNA The presence of these lesions was initially found in poly(dA), poly(dA-dT), or salmon testis DNA upon exposure to γ-rays under anoxic conditions, where α-dA was a major lesion formed at a level of ~1.5%. Additionally, α-dG was recently detected at the levels of 2.2–2.7 lesions per 10^6 nucleosides in mouse pancreatic tissues and commercially available calf thymus DNA.[9] It is worth noting that the levels of α-dG are higher than those of the (5′S) diastereomer of 8,5′-cyclo-2′-deoxyguanosine (*S*-cdG),[9] an oxidatively induced DNA lesion that is known to accumulate with aging.[10]

The presence of DNA damage has the potential to result in cell cycle arrest in dividing cells, which provides time for the DNA repair machinery to resolve the damage in order to maintain genomic stability.[11–15] While some DNA lesions may be successfully repaired, others are more resistant to repair and may result in sustained stalling of the replication fork.

In order to avoid apoptosis due to replication blockage, cells are equipped with translesion synthesis (TLS) DNA polymerases, which encompass polymerases η, ι, κ, and Rev1 in the Y-family, and polymerase ζ in the B-family. [6,7] Owing to their more spacious active sites, these polymerases are capable of bypassing various DNA lesions, with some having the ability to bypass certain DNA lesions with accuracy and efficiency that are similar or even better than bypassing unmodified nucleosides. [16–21] Specifically, polymerase η (Pol η) has been shown to preferentially insert the correct nucleotide, dAMP, opposite the UV-induced thymine–thymine cyclobutane pyrimidine dimers with high efficiency.[16,19,20,22,23] This has been established as the major role of Pol η, and its importance is manifested in patients suffering from the variant form of xeroderma pigmentosum (XPV). These individuals are deficient in Pol η and exhibit elevated sunlight-induced mutagenesis along with increased susceptibility toward developing skin cancer.[22–24] Although this is the main recognized role of Pol η, the polymerase can bypass many other DNA lesions with different degrees of fidelity and efficiency.[25–29]

Previous studies have investigated the impact of α-dN lesions on DNA replication in *Escherichia coli*. Shimizu et al.[30] found that α-dA highly blocked DNA replication, with the relative bypass efficiency (RBE) being 20% when compared to that of dA. In addition, Amato et al.[9] examined the recognition of the four α-nucleosides by the replication machinery of *E. coli* cells that are proficient in translesion synthesis or absent of one or more of the SOS-induced DNA polymerases. It was observed that, in wild-type cells, α-dA also strongly blocked DNA replication with a RBE of 24%, while α-dT, α-dC, and α-dG had significantly lower RBEs (1–3%).[9] Additionally, upon SOS induction, the RBE values for all four of the α-dN lesions were significantly elevated, with the two purine α-nucleosides being less blocking to DNA replication than the pyrimidine counterparts.[9] Moreover, in SOS-induced cells, the absence of Pol V, an orthologue of human Pol η, led to substantial decreases in RBEs for all α-dN lesions except for α-dA. The depletion of this polymerase in SOS-induced cells also led to a substantial drop in T → A mutation for α-dT and abolished the C → G mutation for α-dC. Together, these results unveiled the importance of Pol V in replicative bypass of all the α-dN lesions except α-dA. Thus, in the present study, we focus on the biochemical characterizations about the efficiency and fidelity of Pol η-mediated nucleotide insertion opposite the α-dN lesions.

Experimental Procedures

Materials

Human Pol η, Pol κ, and yeast Pol ζ, (comprising the Rev3 and Rev7 subunits) were purchased from Enzymax (Lexington, KY), and the recombinant full-length human Pol ι was kindly provided by Professor Linlin Zhao (Central Michigan University). All other enzymes were obtained from New England BioLabs (Ipswich, MA), and unmodified oligodeoxyribonucleotides (ODNs) were acquired from Integrated DNA Technologies (Coralville, IA). [γ-^{32}P]-ATP was obtained from PerkinElmer (Boston, MA), and all other chemicals were from Sigma-Aldrich (St. Louis, MO).

Substrate Preparation

The 12-mer α-dN-containing ODNs d(ATGGCGXGCTAT), where X designates the α-dA, α-dT, α-dC, or α-dG, were previously synthesized.[9] The 20-mer lesion-containing ODNs were generated by ligating the 12-mer α-dN-containing ODN (Figure 1) to an 8-mer ODN d(GATCCTAG) in the presence of a 27-mer scaffold d(GTAGCTAGGATCATAGCACGCCATTAG), as previously described.[31] The ligation products were then purified by polyacrylamide gel electrophoresis (PAGE) and annealed to a 13-mer primer (Figure 1).

Primer Extension Assays

Primer extension assays were performed under standing-start conditions, where the primer stops right before the site of the lesion or its corresponding unmodified nucleoside (Figure 1).[32] The primer–template complex containing the 13-mer primer (at a final concentration of 10 nM) was incubated in a reaction buffer at 37 °C for 1 h with various concentrations of human Pol η, κ, and ι, or for 5 h with yeast Pol ζ, (Figure 2 and Figures S1–S3) and all four dNTPs (250 μM each). The reaction buffer contained 25 mM potassium phosphate (pH 7.0), 5 mM $MgCl_2$,5 mM DTT, 100 μg/mL BSA, and 10% glycerol. An equal volume of formamide gel-loading buffer [80% formamide, 10 mM EDTA (pH 8.0), 1 mg/mL xylene cyanol, and 1 mg/mL bromophenol blue] was added to terminate the reaction. The reaction mixtures were subsequently resolved on a 20% (19:1) denaturing polyacrylamide gel and the gel band intensities analyzed using a Typhoon 9410 Variable Mode Imager (Amersham Biosciences Co.).

A 14-mer primer was also employed for primer extension assays involving yeast Pol ζ, where the primer contained the correct nucleoside opposite the α-dN or the corresponding unmodified dN in the template. Primer extension assays were then carried out with the primer–template complexes (at a final concetration of 10 nM) and yeast Pol ζ, under otherwise identical conditions as described above (Figure S4).

Steady-State Kinetic Assay

Steady-state kinetic assays were performed under standing-start conditions following previously published procedures, where the reaction conditions were optimized so that the extent of nucleotide incorporation was less than 20%.[32] The control or lesion-containing primer–template complexes (final concentration of 10 nM) were incubated at 37 °C for 10 min with the above-mentioned reaction buffer, 5 nM human Pol η, and various concentrations of individual dNTPs (Figure 3 and Figure S5). The steady-state kinetic assays were also performed for α-dG- and the corresponding dG-bearing primer–template complexes (at a final concentration of 10 nM) with 5 nM human Pol κ under the above-mentioned conditions (Figure S6). The reactions were terminated by adding an equal volume of formamide gel-loading buffer, and the resulting mixtures were then resolved on a 20% (19:1) denaturing PAGE, and the gel-band intensities were quantified by phosphorimaging analysis.

From the gel images, we first determined the observed rate for nucleotide incorporation, V_{obs}, by dividing the quantified amount of product with the incubation time (i.e., 10

min).[33,34] We then determined the kinetic parameters (i.e., V_{max} and K_m) for nucleotide incorporation by plotting V_{obs} as a function of dNTP concentration and by fitting the data according to the Michaelis–Menten equation using Origin 6.0 (Origin-Lab).[32]

The k_{cat} values were calculated by dividing V_{max} with the concentration of human Pol η used. The efficiency of nucleotide incorporation was determined by the ratio of k_{cat}/K_m, and the frequency of incorrect nucleotide insertion (f_{inc}) was calculated from the ratio of k_{cat}/K_m obtained for the insertion of incorrect nucleotide over that for the correct nucleotide incorporation.[32] In this regard, it is of note that, because the concentration ratio between the primer/template complex (10 nM) and DNA polymerase (5 nM) is relatively low, the nucleotide incorporation may proceed through an initial burst followed by a steady-state reaction. Nevertheless, the k_{cat}/K_m values for nucleotide insertion determined from these measurements reflect the miscoding potentials for the α-dN lesions and indicate the degrees to which these lesions stall translesion synthesis polymerases.

Results

The main objective of the present study was to investigate the replicative bypass of α-dN lesions by TLS DNA polymerases, with the emphasis being placed on human Pol η.

Primer Extension Assay

We first conducted primer extension assays to assess the abilities of human Pol η, κ, ι, and yeast Pol ζ to extend a 13-mer primer in the presence of a 20-mer template containing an unmodified dN or site-specifically inserted α-dN (Figure 1). The results showed that, in the presence of all four dNTPs, human Pol η was the only TLS polymerase capable of bypassing successfully all four α-dN lesions and extending the primer to the end of the template (Figure 2 and Figures S1–S3). Human Pol κ generated more full-length products for the α-dG substrate than substrates housing other α-dN lesions, though the main product observed was a shorter 19-mer product instead of the full-length 20-mer product (Figure S1). Interestingly, the amount of Pol κ-generated full-length extension product for the α-dG substrate (~4.2%) was similar to that observed for the primer extension catalyzed by human Pol η. Human Pol κ was also capable of generating a small amount (~1%) of full-length extension product when bypassing α-dA and α-dT; the polymerase, however, failed to bypass α-dC (Figure S1). Human Pol ι was able to insert a nucleotide opposite α-dA, α-dC, and α-dG but was unable to generate full-length extension products, and no nucleotide incorporation opposite α-dT was observed (Figure S2). Finally, no incorporation or extension was detected for the yeast Pol ζ-mediated bypass of any of the α-dN lesions (Figure S3).

We next conducted primer extension assays to assess if yeast Pol ζ is capable of extending the primer after the correct nucleotide is incorporated opposite the lesion. Our results showed that, while yeast Pol ζ could generate full-length extension products for the unmodified substrates, the polymerase was not able to extend the mismatched primer for any of the α-dN-bearing substrates (Figure S4).

Steady-State Kinetic Analysis

Steady-state kinetic assays were next performed to assess the efficiency and fidelity of human Pol η in inserting nucleotides opposite the α-dN lesions (Figure 3 and Table 1). These results revealed that the presence of α-nucleosides significantly reduces the efficiency for human Pol η-mediated insertion of the correct nucleotide, with the extents of reduction being markedly greater for α-dG, α-dT, and α-dC (4.9%, 3.0%, and 0.55%, repectively) than for α-dA (21%, all relative to nucleotide incorporation opposite the corresponding unmodified nucleoside, Figure 4).

Next, we investigated the differences in the human Pol η-mediated incorporation of incorrect nucleotides opposite the four α-dN lesions. The results showed that the polymerase misincorporates dTMP opposite α-dT and dCMP opposite α-dC at frequencies of 66% and 24%, respectively (Figure 4). Interestingly, α-dA and α-dG directed very low frequencies of nucleotide misincorporation (Figures 4 and 5), revealing that human Pol η has a higher fidelity when bypassing these purine lesions relative to their pyrimidine counterparts.

The above primer extension assay results revealed Pol κ's capability in bypassing readily the α-dG-containing substrate; thus, we also performed the steady-state kinetic measurements for the human Pol κ-mediated nucleotide incorporation opposite α-dG and dG in the corresponding unmodified substrate (Figure S6). Our results showed that human Pol κ's efficiency at incorporating the correct nucleotide, dCMP, opposite α-dG was significantly reduced relative to the corresponding nucleotide insertion opposite the unmodified dG (0.064%, Table S1). Additionally, no detectable incorporation of dAMP opposite α-dG could be observed even with the use of 2 mM dATP, though moderate frequencies of misincorporation of dTMP and dGMP were observed (18% and 17%, respectively, Table S1).

Discussion

In the present study, we investigated the replicative bypass of the four α-nucleosides by human Pol η, κ, ι, and yeast Pol ζ. Results from the primer extension assays revealed the capabilities of the different TLS polymerases in bypassing these lesions and generating full-length extension products. In the mutual presence of all four dNTPs, human Pol η was the only polymerase capable of bypassing all four α-dN lesions and producing full-length replication products (Figure 2). Human Pol κ was capable of bypassing α-dA, α-dT, and α-dG but not α-dC (Figure S1). Furthermore, human Pol κ generated much more extension products for the template containing an α-dG than those carrying an α-dA or α-dT, and the amount of full-length extension product generated for the α-dG substrate was comparable to that generated by human Pol η. Human Pol ι was unable to generate full-length replication products, as reflected by the lack of capability of this polymerase in extending the primer to the end of the templates harboring the α-dN lesions (Figure S2). Additionally, yeast Pol ζ failed to insert any nucleotide opposite any of the α-dN lesions or extend past the damage (Figures S3 and S4).

Our steady-state kinetic assays revealed that the efficiencies and fidelities of human Pol η-mediated nucleotide incorporations depend on the identities of the α-nucleosides. In

particular, when considering the relative efficiencies (k_{cat}/K_m) of correct nucleotide incorporation opposite the α-dN lesions over their unmodified counterparts, we found that the magnitudes of decrease in efficiencies for nucleotide incorporation followed the order of α-dA > α-dG > α-dT > α-dC. Additionally, we measured the frequencies of incorrect nucleotide incorporation opposite the α-dN lesions. Human Pol η was found to be highly accurate when bypassing the purine lesions, i.e. α-dA and α-dG, with the incorrect nucleotides being incorporated at relatively low frequencies. However, replicative bypass of the pyrimidine lesions, i.e. α-dT and α-dC, led to high frequencies of misincorporation of dTMP and dCMP. The exact reason behind the differences in fidelity for human Pol η-mediated nucleotide incorporation opposite the different α-dN lesions is not clear and warrants further investigations in the future.

Our primer extension results revealed that human Pol η- and human Pol κ-mediated primer extension yielded similar amounts of full-length products for the α-dG substrate. Hence, steady-state kinetic assays were also performed for this lesion with human Pol κ. While both polymerases preferentially incorporate the correct nucleotide opposite the lesion, human Pol η exhibits a signficianly higher effieincy of dCMP incorporation (k_{cat}/K_m) than that of human Pol κ (6.8×10^{-2} $\mu M^{-1}min^{-1}$ vs 2.2×10^{-4} $\mu M^{-1}min^{-1}$ (Table 1 and Table S1). The same trend also holds true for the incorporation of the incorrect nucleotides (Table 1 and Table S1). These results together suggest that, among the four polymerases tested, human Pol η is the most efficient in bypassing the α-dN lesions.

These results are in keeping with previous findings about the effects that the α-dN lesions have on DNA replication *in vitro* and in *E. coli* cells. In this vein, Ide and co-workers[35] investigated the *E. coli* Pol I-mediated bypass of α-dA using primer extension and steady-state kinetic assays. They determined that α-dA blocked DNA synthesis, though Pol I could extend the primer beyond the lesion.[35] They also determined the order of insertion frequency of individual nucleotides opposite α-dA to be dTMP > dCMP > dAMP,[35] whereas Pol I was unable to incorporate dGMP opposite the lesion.[35] Other studies investigating the effects of the α-dN lesions on DNA replication in *E. coli* found that α-dA stalls replication with a RBE of 20–24% relative to the unmodified dA.[9,3]

Additionally, Amato et al[9]. found that α-dT, α-dC, and α-dG strongly blocked DNA replication in wild-type *E. coli* cells with the relative bypass efficiency being only 1–3%. Upon SOS induction, the RBEs for all four α-dN lesions were significantly elevated, with α-dA and α-dG displaying much higher RBEs (>85%) than the two pyrimidine α-nucleosides (15–30%).[9] This is in line with the higher efficiencies of correct nucleotide insertion opposite α-dA and α-dG than α-dC and α-dT (Figure 4). Additionally, the absence of Pol Vin SOS-induced E. *coli* cells led to an abrogation of C → G mutation for α-dC and a marked drop in T → A mutation for α-dT,[9] which is in agreement with the high preference for human Pol η to misincorporate dCMP and dTMP opposite α-dT and α-dC, respectively. These results suggest that Pol V's recognition of the α-nucleosides is conserved in human Pol η.

Taken together, the results from this study provided important insights into the roles of human Pol η, κ, ι, and yeast Pol ζ in bypassing the α-dN lesions as well as the impact that

these lesions pose on the efficiency and fidelity of human Pol η. In the future, it will be important to determine the roles of the TLS polymerases in bypassing the α-dN lesions in human cells as well as the impacts of these lesions on the efficiency and fidelity of cellular DNA replication. Additionally, future structural studies will provide molecular-level insights about the differential recognitions of the α-dN by human Pol η.

Supplementary Material

Refer to Web version on PubMed Central for supplementary material.

Acknowledgments

Funding: This work was supported by the National Institutes of Health (P01 AG043376).

References

1. Finkel T, Holbrook NJ. Oxidants, oxidative stress and the biology of ageing. Nature. 2000; 408:239–247. [PubMed: 11089981]
2. Harman D. Aging: a theory based on free radical and radiation chemistry. J Gerontol. 1956; 11:298–300. [PubMed: 13332224]
3. Loft S, Poulsen HE. Cancer risk and oxidative DNA damage in man. J Mol Med. 1996; 74:297–312. [PubMed: 8862511]
4. Cooke MS, Evans MD, Dizdaroglu M, Lunec J. Oxidative DNA damage: mechanisms, mutation, and disease. FASEB J. 2003; 17:1195–1214. [PubMed: 12832285]
5. Hoeijmakers JH. DNA damage, aging, and cancer. N Engl J Med. 2009; 361:1475–1485. [PubMed: 19812404]
6. Marnett LJ. Oxyradicals and DNA damage. Carcinogenesis. 2000; 21:361–370. [PubMed: 10688856]
7. Amato NJ, Wang Y. Epimeric 2-deoxyribose lesions: Products from the improper chemical repair of 2-deoxyribose radicals. Chem Res Toxicol. 2014; 27:470–479. [PubMed: 24517165]
8. Lesiak KB, Wheeler KT. Formation of alpha-deoxyadenosine in polydeoxynucleotides exposed to ionizing radiation under anoxic conditions. Radiat Res. 1990; 121:328–337. [PubMed: 2315449]
9. Amato NJ, Zhai Q, Navarro DC, Niedernhofer LJ, Wang Y. In vivo detection and replication studies ofa-anomeric lesions of 2′-deoxyribonucleosides. Nucleic Acids Res. 2015; 43:8314–8324. [PubMed: 26202973]
10. Wang J, Clauson CL, Robbins PD, Niedernhofer LJ, Wang Y. The oxidative DNA lesions 8,5′-cyclopurines accumulate with aging in a tissue-specific manner. Aging Cell. 2012; 11:714–716. [PubMed: 22530741]
11. Houtgraaf JH, Versmissen J, van der Giessen WJ. A concise review of DNA damage checkpoints and repair in mammalian cells. Cardiovasc Revasc Med. 2006; 7:165–172. [PubMed: 16945824]
12. Jackson SP, Bartek J. The DNA-damage response in human biology and disease. Nature. 2009; 461:1071–1078. [PubMed: 19847258]
13. Swenberg JA, Lu K, Moeller BC, Gao L, Upton PB, Nakamura J, Starr TB. Endogenous versus exogenous DNA adducts: Their role in carcinogenesis, epidemiology and risk assessment. Toxicol Sci. 2011; 120:S130–145. [PubMed: 21163908]
14. Harper JW, Elledge SJ. The DNA damage response: ten years after. Mol Cell. 2007; 28:739–745. [PubMed: 18082599]
15. Sancar A, Lindsey-Boltz LA, Unsal-Kacmaz K, Linn S. Molecular mechanisms of mammalian DNA repair and the DNA damage checkpoints. Annu Rev Biochem. 2004; 73:39–85. [PubMed: 15189136]
16. Chang DJ, Cimprich KA. DNA damage tolerance: when it's OK to make mistakes. Nat Chem Biol. 2009; 5:82–90. [PubMed: 19148176]

17. Lehmann AR, Niimi A, Ogi T, Brown S, Sabbioneda S, Wing JF, Kannouche PL, Green CM. Translesion synthesis: Y-family polymerases and the polymerase switch. DNA Repair. 2007; 6:891–899. [PubMed: 17363342]
18. Jarosz DF, Godoy VG, Delaney JC, Essigmann JM, Walker GC. A single amino acid governs enhanced activity of DinB DNA polymerases on damaged templates. Nature. 2006; 439:225–228. [PubMed: 16407906]
19. Johnson RE, Prakash S, Prakash L. Efficient bypass of a thymine-thymine dimer by yeast DNA polymerase, Pol77. Science. 1999; 283:1001–1004. [PubMed: 9974380]
20. Masutani C, Kusumoto R, Yamada A, Dohmae N, Yokoi M, Yuasa M, Araki M, Iwai S, Takio K, Hanaoka F. The XPV (xeroderma pigmentosum variant) gene encodes human DNA polymerase η. Nature. 1999; 399:700–704. [PubMed: 10385124]
21. Yuan B, Cao H, Jiang Y, Hong H, Wang Y. Efficient and accurate bypass of N^2-(1-carboxyethyl)-2′-deoxyguanosine by DinB DNA polymerase *in vitro* and *in vivo*. Proc Natl Acad Sci U S A. 2008; 105:8679–8684. [PubMed: 18562283]
22. Biertumpfel C, Zhao Y, Kondo Y, Ramon-Maiques S, Gregory M, Lee JY, Masutani C, Lehmann AR, Hanaoka F, Yang W. Structure and mechanism of human DNA polymerase eta. Nature. 2010; 465:1044–1048. [PubMed: 20577208]
23. Limoli CL, Giedzinski E, Morgan WF, Cleaver JE. Polymerase η deficiency in the xeroderma pigmentosum variant uncovers an overlap between the S phase checkpoint and double-strand break repair. Proc Natl Acad Sci U S A. 2000; 97:7939–7946. [PubMed: 10859352]
24. Cleaver JE. Cancer in xeroderma pigmentosum and related disorders of DNA repair. Nat Rev Cancer. 2005; 5:564–573. [PubMed: 16069818]
25. Gu C, Wang Y. LC-MS/MS identification and yeast polymerase η bypass of a novel γ-irradiation-induced intrastrand crosslink lesion G[8–5]C. Biochemistry. 2004; 43:6745–6750. [PubMed: 15157108]
26. You C, Swanson AL, Dai X, Yuan B, Wang J, Wang Y. Translesion synthesis of 8,5′-cyclopurine-2′-deoxynucleosides by DNA polymerases η, ι, and ζ. J Biol Chem. 2013; 288:28548–28556. [PubMed: 23965998]
27. Williams NL, Wang P, Wu J, Wang Y. In vitro lesion bypass studies of O^4-Alkylthymidines with human DNA polymerase η. Chem Res Toxicol. 2016; 29:669–675. [PubMed: 27002924]
28. Williams NL, Wang P, Wang Y. Replicative bypass of O^2-alkylthymidine lesions *in vitro*. Chem Res Toxicol. 2016; 29:1755–1761. [PubMed: 27611246]
29. Wu J, Wang P, You C, Williams NL, Wang Y. Translesions synthesis of O^4-alkylthymidine lesions in human cells. Nucleic Acids Res. 2016; 44:9256–9265. [PubMed: 27466394]
30. Shimizu H, Yagi R, Kimura Y, Makino K, Terato H, Ohyama Y, Ide H. Replication bypass and mutagenic effect of alpha-deoxyadenosine site-specifically incorporated into single-stranded vectors. Nucleic Acids Res. 1997; 25:597–603. [PubMed: 9016601]
31. Gu C, Wang Y. LC-MS/MS identification and yeast polymerase η bypass of a novel γ-irradiation-induced intrastrand crosslink lesion G [8–5]C. Biochemistry. 2004; 43:6745–6750. [PubMed: 15157108]
32. Goodman MF, Creighton S, Bloom LB, Petruska J, Kunkel TA. Biochemical basis of DNA replication fidelity. Crit Rev Biochem Mol Biol. 1993; 28:83–126. [PubMed: 8485987]
33. Johnson RE, Washington MT, Prakash S, Prakash L. Fidelity of human DNA polymerase η. J Biol Chem. 2000; 275:7447–7450. [PubMed: 10713043]
34. Washington MT, Johnson RE, Prakash S, Prakash L. Accuracy of thymine-thymine dimer bypass by Saccharomyces cerevisiae DNA polymerase η. Proc Natl Acad Sci U S A. 2000; 97:3094–3099. [PubMed: 10725365]
35. Ide H, Yamaoka T, Kimura Y. Replication of DNA templates containing the alpha-anomer of deoxyadenosine, a major adenine lesion produced by hydroxyl radicals. Biochemistry. 1994; 33:7127–7133. [PubMed: 8003479]

Abbreviations

ROS	reactive oxygen species
TLS	translesion synthesis
Pol	polymerase
ODN	oligodeoxyribonucleotide
PAGE	polyacrylamide gel electrophoresis
XPV	xeroderma pigmentosum variant

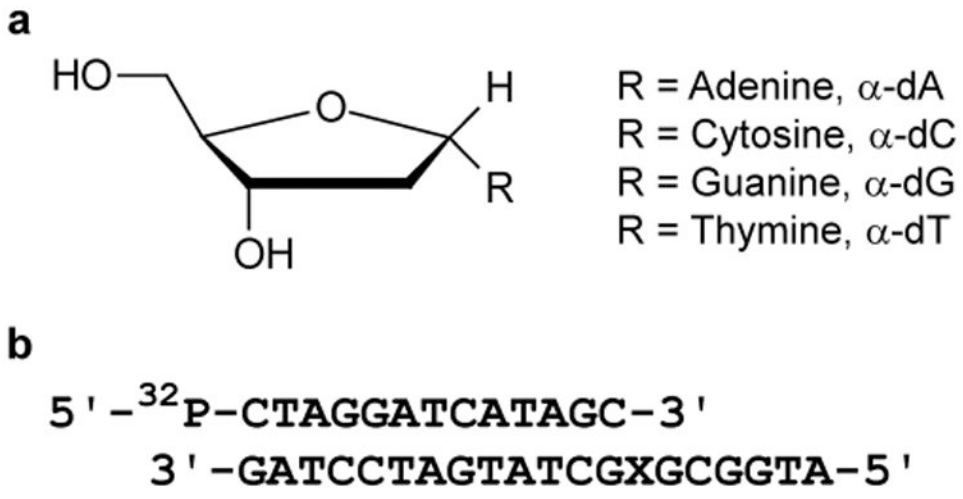

Figure 1.

(a) Structures of the α-dN lesions examined in this study and (b) the primer–template complex used for the *in vitro* primer extension and steady-state kinetic assays. X represents the α-dN lesions and their corresponding unmodified nucleosides.

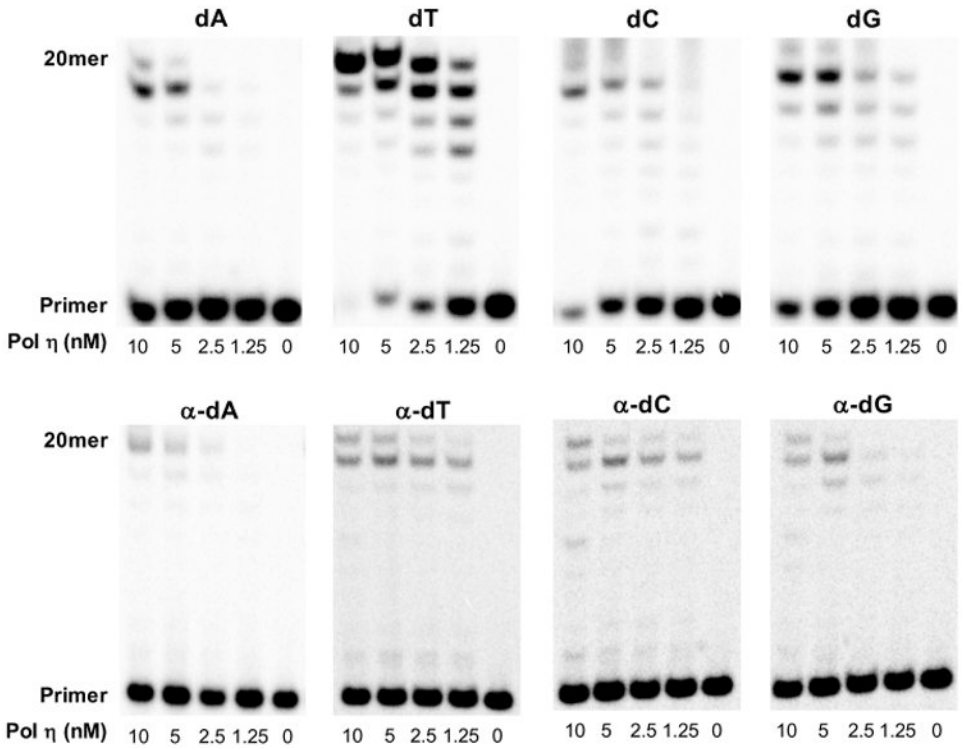

Figure 2.

Representative gel images from the primer extension assays under standing-start conditions for primer–template complexes harboring an α-nucleoside or its unmodified counterpart with human Pol η at final concentrations of 0, 1.25, 2.5, 5.0, and 10.0 nM. The final concentration of the primer–template complex was 10 nM.

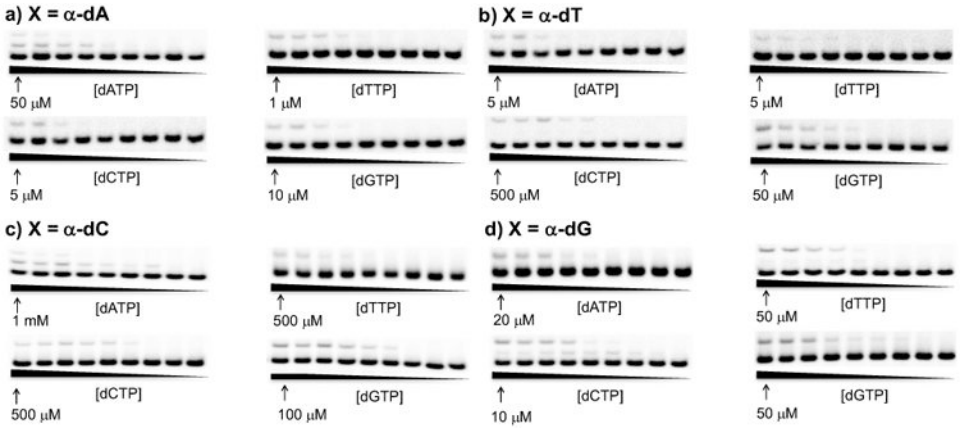

Figure 3.

Representative gel images for steady-state kinetic assays measuring the individual nucleotide incorporation opposite α-dA (a), α-dT (b), α-dC (c), and α-dG (d) with human Pol η. The final concentration of the primer–template complex was 10 nM, and the final concentration of human Pol η was 5 nM. The highest concentrations of individual dNTPs used are indicated in the figure, and the concentration ratio between neighboring lanes was 0.50.

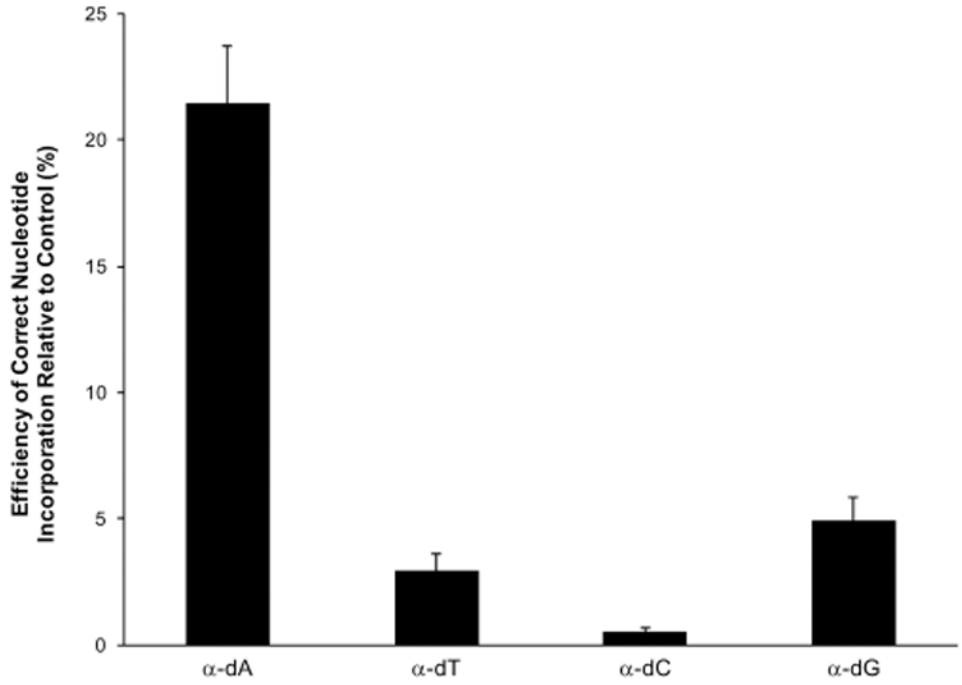

Figure 4.

Efficiencies for the human Pol η-catalyzed insertion of the correct nucleotide opposite α-dA, α-dT, α-dC, and α-dG (relative to unmodified substrates). The results represent the mean ± standard deviation of results from at least three independent measurements.

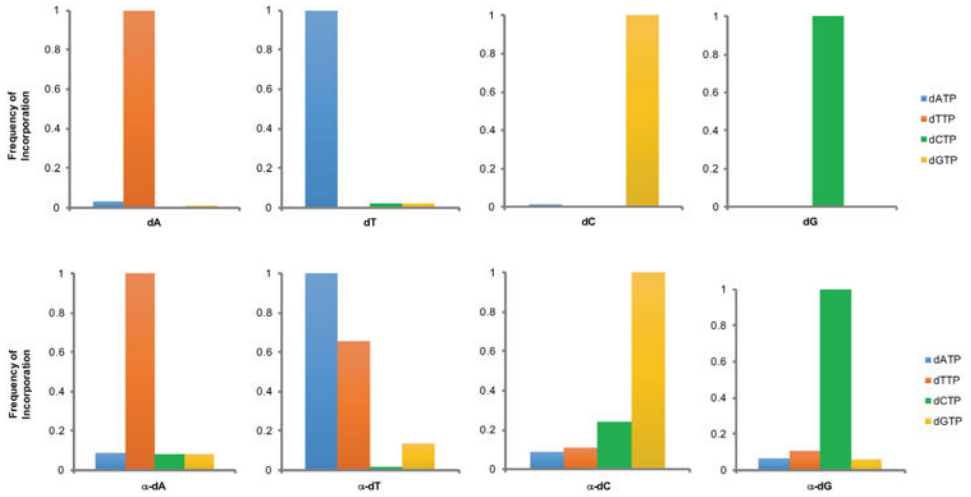

Figure 5.

Relative efficiencies for the Pol η-mediated nucleotide incorporation opposite dA, dT, dC, dG, α-dA, α-dT, α-dC, and α-dG.

Table 1

Steady-State Kinetic Parameters for Human Pol η-Mediated Incorporation of Individual dNTPs Opposite the α-dA, α-dT, α-dC, α-dG, and unmodified dA, dT, dC, and dG Substrates[a]

dNTP	k_{cat} (min^{-1})	K_m (μM)	k_{cat}/K_m ($\mu M^{-1}min^{-1}$)	f_{inc}[b]
		Undamaged dA Substrate		
dTTP	$2.1 \times 10^{-2} \pm 4 \times 10^{-3}$	$7.7 \times 10^{-2} \pm 2 \times 10^{-2}$	$2.8 \times 10^{-1} \pm 3 \times 10^{-2}$	1.0
dGTP	$5.7 \times 10^{-2} \pm 3 \times 10^{-3}$	25 ± 4	$2.3 \times 10^{-3} \pm 3 \times 10^{-4}$	8.2×10^{-3}
dCTP	$5.7 \times 10^{-2} \pm 6 \times 10^{-3}$	57 ± 10	$1.0 \times 10^{-3} \pm 1 \times 10^{-4}$	3.7×10^{-3}
dATP	$3.5 \times 10^{-2} \pm 3 \times 10^{-3}$	$4.1 \pm 2 \times 10^{-1}$	$8.7 \times 10^{-3} \pm 2 \times 10^{-3}$	3.1×10^{-2}
		α-dA		
dTTP	$2.2 \times 10^{-2} \pm 7 \times 10^{-4}$	$3.7 \times 10^{-1} \pm 2 \times 10^{-2}$	$6.0 \times 10^{-2} \pm 1 \times 10^{-3}$	1.0
dGTP	$2.4 \times 10^{-2} \pm 3 \times 10^{-3}$	$4.9 \pm 7 \times 10^{-1}$	$4.9 \times 10^{-3} \pm 2 \times 10^{-4}$	8.2×10^{-2}
dCTP	$6.2 \times 10^{-3} \pm 6 \times 10^{-4}$	$1.3 \pm 2 \times 10^{-1}$	$5.0 \times 10^{-3} \pm 2 \times 10^{-5}$	8.3×10^{-2}
dATP	$1.9 \times 10^{-2} \pm 3 \times 10^{-3}$	$3.7 \pm 5 \times 10^{-1}$	$5.2 \times 10^{-3} \pm 2 \times 10^{-3}$	8.7×10^{-2}
		Undamaged dT Substrate		
dTTP	$1.1 \times 10^{-2} \pm 2 \times 10^{-3}$	10 ± 2	$1.1 \times 10^{-3} \pm 2 \times 10^{-4}$	2.1×10^{-3}
dGTP	$2.7 \times 10^{-2} \pm 4 \times 10^{-3}$	$2.3 \pm 6 \times 10^{-1}$	$1.2 \times 10^{-2} \pm 1 \times 10^{-3}$	2.3×10^{-2}
dCTP	$2.7 \times 10^{-2} \pm 5 \times 10^{-3}$	$2.4 \pm 1 \times 10^{-1}$	$1.1 \times 10^{-2} \pm 2 \times 10^{-3}$	2.3×10^{-2}
dATP	$1.5 \times 10^{-2} \pm 3 \times 10^{-3}$	$3.0 \times 10^{-2} \pm 9 \times 10^{-4}$	$5.0 \times 10^{-1} \pm 8 \times 10^{-2}$	1.0
		α-dT		
dTTP	$7.6 \times 10^{-3} \pm 8 \times 10^{-4}$	$7.8 \times 10^{-1} \pm 1 \times 10^{-1}$	$9.8 \times 10^{-3} \pm 1 \times 10^{-3}$	6.6×10^{-1}
dGTP	$1.1 \times 10^{-1} \pm 1 \times 10^{-2}$	55 ± 8	$2.0 \times 10^{-3} \pm 2 \times 10^{-4}$	1.4×10^{-1}
dCTP	$2.1 \times 10^{-2} \pm 1 \times 10^{-3}$	75 ± 6	$2.8 \times 10^{-4} \pm 2 \times 10^{-5}$	1.8×10^{-2}
dATP	$3.1 \times 10^{-2} \pm 4 \times 10^{-3}$	$2.1 \pm 5 \times 10^{-1}$	$1.5 \times 10^{-2} \pm 2 \times 10^{-3}$	1.0
		Undamaged dC Substrate		
dTTP	$6.2 \times 10^{-2} \pm 9 \times 10^{-3}$	39 ± 9	$1.6 \times 10^{-3} \pm 2 \times 10^{-4}$	3.2×10^{-3}
dGTP	$5.5 \times 10^{-2} \pm 5 \times 10^{-3}$	$1.2 \times 10^{-1} \pm 3 \times 10^{-2}$	$4.9 \times 10^{-1} \pm 1 \times 10^{-1}$	1.0
dCTP	$5.4 \times 10^{-2} \pm 8 \times 10^{-3}$	47 ± 9	$1.2 \times 10^{-3} \pm 2 \times 10^{-4}$	2.4×10^{-3}
dATP	$6.9 \times 10^{-2} \pm 9 \times 10^{-3}$	11 ± 1	$6.1 \times 10^{-3} \pm 7 \times 10^{-4}$	1.2×10^{-2}
		α-dC		
dTTP	$2.9 \times 10^{-2} \pm 2 \times 10^{-4}$	100 ± 20	$2.9 \times 10^{-4} \pm 6 \times 10^{-5}$	1.1×10^{-1}
dGTP	$3.9 \times 10^{-2} \pm 2 \times 10^{-3}$	15 ± 2	$2.7 \times 10^{-3} \pm 2 \times 10^{-4}$	1.0
dCTP	$1.2 \times 10^{-2} \pm 4 \times 10^{-4}$	18 ± 2	$6.4 \times 10^{-4} \pm 6 \times 10^{-5}$	2.4×10^{-1}
dATP	$3.9 \times 10^{-2} \pm 4 \times 10^{-3}$	170 ± 20	$2.4 \times 10^{-4} \pm 4 \times 10^{-5}$	8.8×10^{-2}
		Undamaged dG Substrate		
dTTP	$4.8 \times 10^{-2} \pm 8 \times 10^{-4}$	17 ± 4	$2.9 \times 10^{-3} \pm 6 \times 10^{-4}$	2.1×10^{-3}
dGTP	$8.8 \times 10^{-2} \pm 1 \times 10^{-3}$	300 ± 40	$3.0 \times 10^{-4} \pm 3 \times 10^{-5}$	2.2×10^{-4}
dCTP	$5.7 \times 10^{-2} \pm 7 \times 10^{-3}$	$4.1 \times 10^{-2} \pm 8 \times 10^{-3}$	$1.4 \pm 2 \times 10^{-1}$	1.0
dATP	$5.3 \times 10^{-2} \pm 4 \times 10^{-3}$	22 ± 1	$2.4 \times 10^{-3} \pm 2 \times 10^{-4}$	1.8×10^{-3}

dNTP	k_{cat} (min^{-1})	K_m (μM)	k_{cat}/K_m ($\mu M^{-1}min^{-1}$)	f_{inc} [b]
		a-dG		
dTTP	$3.4 \times 10^{-2} \pm 4 \times 10^{-3}$	$4.9 \pm 9 \times 10^{-1}$	$7.2 \times 10^{-3} \pm 2 \times 10^{-3}$	1.1×10^{-1}
dGTP	$3.1 \times 10^{-2} \pm 5 \times 10^{-3}$	7.8 ± 2	$4.0 \times 10^{-3} \pm 3 \times 10^{-4}$	5.9×10^{-2}
dCTP	$4.3 \times 10^{-2} \pm 2 \times 10^{-3}$	$6.4 \times 10^{-1} \pm 9 \times 10^{-2}$	$6.8 \times 10^{-2} \pm 1 \times 10^{-2}$	1.0
dATP	$3.9 \times 10^{-2} \pm 4 \times 10^{-3}$	8.9 ± 1	$4.4 \times 10^{-3} \pm 2 \times 10^{-4}$	6.5×10^{-2}

[a] Shown are the mean ± standard deviation of results from at least three independent measurements.

[b] Frequency of nucleotide misincorporation = [k_{cat}/K_m (incorrect nucleotide)]/[k_{cat}/K_m (correct nucleotide)].